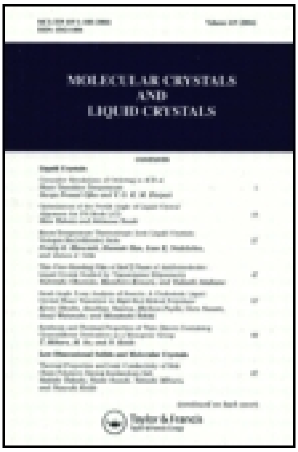

Molecular Crystals and Liquid Crystals
Publication details, including instructions for authors and subscription information:
http://www.tandfonline.com/loi/gmcl20

Elaboration of Side-Chain Liquid-Crystalline Elastomers and Study of Their Swelling Behavior in Anisotropic Solvents

N. Bouchikhi [a], F. Semdani [a], L. Alachaher Bedjaoui [a] & U. Maschke [b]

[a] Laboratoire de Recherche sur les Macromolécules, Faculté des Sciences, Université de Tlemcen, BP119, 13000, Tlemcen, Algeria

[b] Unité Matériaux et Transformations (UMET), UMR 8207—CNRS, Université Lille 1 - Sciences et Technologies, 59655, Villeneuve d'Ascq Cedex, France

Version of record first published: 15 May 2012.

To cite this article: N. Bouchikhi, F. Semdani, L. Alachaher Bedjaoui & U. Maschke (2012): Elaboration of Side-Chain Liquid-Crystalline Elastomers and Study of Their Swelling Behavior in Anisotropic Solvents, Molecular Crystals and Liquid Crystals, 560:1, 159-169

To link to this article: http://dx.doi.org/10.1080/15421406.2012.663196

Mol. Cryst. Liq. Cryst., Vol. 560: pp. 159–169, 2012
Copyright © Taylor & Francis Group, LLC
ISSN: 1542-1406 print/1563-5287 online
DOI: 10.1080/15421406.2012.663196

Elaboration of Side-Chain Liquid-Crystalline Elastomers and Study of Their Swelling Behavior in Anisotropic Solvents

N. BOUCHIKHI,[1] F. SEMDANI,[1] L. ALACHAHER BEDJAOUI,[1]
AND U. MASCHKE[2,*]

[1]Laboratoire de Recherche sur les Macromolécules, Faculté des Sciences,
Université de Tlemcen, BP119, 13000 Tlemcen, Algeria
[2]Unité Matériaux et Transformations (UMET), UMR 8207—CNRS, Université
Lille 1 - Sciences et Technologies, 59655 Villeneuve d'Ascq Cedex, France

A poly [6-(4′-cyanophenyl-4″-phenoxy) alkyl acrylate] side chain liquid crystalline elastomer and a poly [n-butylacrylate] network were synthesized via photopolymerization using 1,6-hexanediol diacrylate as a crosslinking agent. The materials obtained were characterized by differential scanning calorimetry and polarized optical microscopy. In particular, the latter method allowed to follow the swelling behavior of the polymer networks in a low molar weight liquid crystal (LC) and to observe the formation of LC gels. In the case of the anisotropic network, a stable nematic gel phase and a miscibility gap were observed, in relationship with the nematic-isotropic transition temperatures of both LC-solvent and LC-gel. The experimental phase diagrams were well reproduced by a mean field model combining the Flory-Rehner model for isotropic mixing and the Maier Saupe theory for nematic ordering.

Keywords Side chain liquid crystalline elastomers; photo-polymerization; swelling; phase diagram

1. Introduction

During the last two decades, liquid crystalline (LC) polymers have been systematically studied due to their properties making them useful for a large number of applications [1, 2]. The interest of these materials lies in the combination of the properties typical for conventional monomeric LCs with those peculiar to polymers [3]. Note that two different classes of LC polymers exist: main-chain and side-chain (comb-like). In side-chain LC polymers, the pendant mesogenic groups are linked to a linear polymer backbone, by an (often flexible) spacer. Main-chain LC polymers are built up by combining rod-like mesogenic fragments and flexible moieties in alternating succession.

LC elastomers (LCEs) are polymeric networks containing covalently bound mesogenic groups, in a main-chain, side-chain or mixed main-chain/side-chain configuration [4–9]. Their synthesis was reported essentially by Finkelmann et al. [10] using mainly

---

[*] Address correspondence to U. Maschke, Unité Matériaux et Transformations (UMET), UMR 8207 - CNRS, Université Lille 1 - Sciences et Technologies, 59655 Villeneuve d'Ascq Cedex, France. Phone: +33-3-20 33 63 81; Fax: +33-3-20 43 43 45. E-mail: ulrich.maschke@univ-lille1.fr

polysiloxanes, polyacrylates, polymethacrylates, and polyurethanes as polymer backbone. This relatively new class of LC has rapidly expanded because they give rise to interesting macroscopic features [11–13].

Several theoretical [14–18] and experimental studies [19, 20] have been devoted to the interactions of LCE with solvents in which LC ordering is possible. The potential applications of nematic elastomers include low frequency, large amplitude actuators and transducers driven by weak electric and optical fields, and components of artificial muscles (biomimetic sensors) [21, 22]. It is evident that the most attractive applications would involve a strong response to a low electric field. This has led to intensive investigations of systems composed of LCEs swollen with low molecular mass nematic materials. Network formation can be induced chemically by copolymerization of polymer chains with a given density of reactive sites and the presence of a crosslinking agent. Alternatively, polymerization can be accomplished by addition of a photoinitiator to the system and subsequent exposure to UV light.

The process of network swelling in low molecular weight solvents has been subject of intensive studies for several decades [23], and particularly the phase behavior of polymer network/solvent systems possessing nematicity has attracted much attention mainly from the theoretical viewpoint [24, 25], because the presence of nematic interactions is expected to yield new and interesting aspects on the phase diagrams. The control of the polymer dissolution, diffusion and swelling processes rely in part on the study of the miscibility behavior of these binary mixtures, providing information about the thermodynamic stability of the coexisting phases as function of temperature and composition.

The present study is focused on experimental and theoretical studies of the phase behavior in binary systems containing high and low molecular weight components (solvent). In the first case a mesogenic solvent and an isotropic polymer network will be considered, and in the second case, both components represent mesogenic moieties. Swelling data were used to establish the phase diagrams in terms of composition and temperature, by means of polarized optical microscopy (POM). The data were analyzed within a theoretical formalism based on a combination of the Flory-Rehner theory [26] of rubber elasticity for polymer solutions and the Maier Saupe theory for nematic ordering [27].

2. Theoretical Considerations

The theoretical considerations used here are based upon a modified double lattice model for isotropic mixing and the Maier-Saupe theory for anisotropic ordering. The free energy density f will be introduced, which is a sum of two terms. The first one, $f^{(i)}$, represents the free energy for isotropic mixing and the second one, $f^{(a)}$, is the free energy for anisotropic ordering. ΔF denotes the free energy for the whole lattice where $\Delta F^{(\mathrm{i})}$ represents the isotropic free energy and $\Delta F^{(\mathrm{a})}$ represents the anisotropic energy, assuming n_0 sites in the lattice. Thus one writes

$$f = f^{(i)} + f^{(a)} = \frac{\Delta F}{n_0 k_B T} = \frac{\Delta F^{(i)} + \Delta F^{(a)}}{n_0 k_B T} \tag{1}$$

The superscripts (i) and (a) stand for isotropic and anisotropic, respectively. The network can be visualized as a single macromolecule with N_t monomers which means that the total number of sites is $n_0 = N_\mathrm{t} + n_1 N_1$. k_B is the Boltzmann constant, and T stands for the absolute temperature.

2.1 The Maier-Saupe Theory for Anisotropic Ordering

Small nematic molecules are aligned along a reference axis in the z direction, exhibiting an angular distribution [28–32]. The nematic free energy density is given by:

$$f^{(a)} = \frac{\Delta F^{(a)}}{n_0 k_B T} = \frac{\varphi_1}{N_1}\Big[-\ln Z + \frac{1}{2}\nu\varphi_1 S^2\Big] \tag{2}$$

φ_1 is the volume fraction of the LC. The normalized partition function Z can be written as:

$$Z = \int e^{-U(\theta)/(k_B T)} d(\cos\theta) \tag{3}$$

where the orientational potential $U(\theta)$ is given by:

$$U(\theta) = -\frac{m}{2}[3\cos^2\theta - 1] \tag{4}$$

m is a mean field parameter representing the potential strength. Minimization of the nematic free energy with respect to S yields

$$m = \varphi_1 \nu S \tag{5}$$

where ν is the Maier-Saupe quadrupole interaction parameter:

$$\nu = 4.54\frac{T_{NI}}{T} \tag{6}$$

where T_{NI} represents the nematic-isotropic transition temperature of the LC. The nematic order parameter S is defined as:

$$S = \frac{1}{2}[3 < \cos^2\theta > -1] \tag{7}$$

$< \ldots >$ denotes the average with respect to the orientation distribution function and θ is the angle between a reference axis and the director of the LC.

2.2 Isotropic Free Energy for a Blend of an LC and a Cross-Linked Polymer

Unlike linear polymers that can be described in agreement with the Flory-Huggins model, a crosslinked polymer network cannot be discussed within this theory due to the existence of chemical crosslinking points which determine the swelling behavior of the polymer, significantly altering the phase behavior [33]. To examine this issue in more detail, the theory of Flory-Rehner [34] will be applied, where the isotropic free energy density is expressed as follows:

$$f^{(i)} = \frac{\Delta F^{(i)}}{n_0 k_B T} = \frac{3\alpha\varphi_0^{2/3}}{2N_C}\big[\varphi_2^{1/3} - \varphi_2\big] + \frac{\beta\varphi_2}{N_C}\ln\Big(\frac{\varphi_2}{\varphi_0}\Big) + \frac{\varphi_1\ln\varphi_1}{N_1} + \chi\varphi_1\varphi_2 \tag{8}$$

where N_C represents the number of monomer units between two consecutive cross-links. φ_1 and φ_2 are the volume fractions of the two species assumed to form an incompressible mixture, where all units occupy the same volume corresponding to that of a lattice site. One has $\varphi_2 = 1 - \varphi_1$. Isotropic mixing of these two molecular species is controlled by the

Flory-Huggins interaction parameter χ. Throughout this paper, N_1 will have a fixed value 1 and the parameter χ will be assumed to be function of the temperature only

$$\chi = A + \frac{B}{T} \tag{9}$$

The constants α and β in equation (8) are model dependent. In the Flory affine network model [35], we have $\alpha = 1$ and $\beta = \frac{2\varphi}{f}$, f being the functionality of the monomers. The phantom network model proposed by James and Guth [36] suggests other values of these parameters. Indeed, they suggest to let $\alpha = 1$ and $\beta = 0$. Recently, Petrovic et al. [37] proposed a linear dependence of α and β on volume fraction of the polymer network of the form $\alpha = \frac{f-2+2\varphi_2}{f}$ and $\beta = \frac{2\varphi_2}{f}$. It should be noted in the latter model that the limit $\varphi_2 \to 1$ corresponds to the Flory affine network model, whereas the limit $\varphi_2 \to 0$ corresponds to the James and Guth phantom model. φ_0 represents the polymer volume fraction at the formation of the network, also known as the reference state volume fraction.

3. Experimental Part

3.1 Materials

The *n*-butyl acrylate (ABu) and the cross-linking agent 1,6 hexanediol diacrylate (HDDA) were obtained from Sigma Aldrich. The photoinitiator 2-hydroxy-2-methyl-1-phenyl-1-propanone (Darocur 1173) and the nematic LC 4-cyano-4′-n-pentylbiphenyl (5CB) were purchased from Ciba and Synthon GmbH (Germany), respectively.

The synthesis of the 6-(4′-cyanophenyl-4″-phenoxy) alkyl acrylate monomer was realized following the method reported by Shibaev et al. [38]. The complete reaction pathway includes four steps and was described in more detail in reference [38].

3.2 Synthesis of the Poly[n-Abu/HDDA] Polymer Network

The isotropic polymer network was fabricated as follows: an Abu/HDDA/Darocur 1173 mixture (94.5/5/0.5 weight% (wt%)) was prepared and stirred mechanically for several hours in order to ensure a uniform distribution of the monomer and the crosslinking agent over the sample volume. The initial mixture was transferred into a Teflon holder and placed inside a reaction chamber filled with nitrogen. Subsequently, the sample was exposed to a UV lamp (Philips TL08) with a wavelength of 365 nm and an intensity of 1,5 mW/cm^2.

The exposure time was fixed to 15 minutes, although 5 minutes was sufficient to achieve a complete conversion of the monomers. After removal from the Teflon mould, the polymer network was obtained as a transparent disk, with a diameter of 2,5 cm and a thickness of 1,5 mm. The network was washed several times in a bath of toluene (good solvent) in order to remove the low molecular species eventually remaining inside the network (monomers and oligomers not attached to the network), dried in air for one day and finally placed under vacuum at room temperature for few hours.

3.3 Synthesis of the Liquid Crystalline Polymer Network

The nematic polymer network was synthesized as follows: 500 mg of the mesogenic acrylic monomer were dissolved in 2 ml of a dimethylsulfoxide-toluene mixture (40–60 volume%) [39]. Then, 5wt% of HDDA was introduced as crosslinking agent and a small amount of photoinitiator (Darocur 1173) was added to the mixture. This blend was stirred mechanically for one hour, introduced into a Teflon mold, and exposed to the above mentioned UV light source under nitrogen atmosphere, for 30 minutes. The isotropic gel was transferred into a bath of dichloromethane and the solvent was renewed several times in order to eliminate unattached species. Then, the solvent quality was gradually decreased via successive exchanges in dichloromethane/methanol mixtures. At the end of the process, the collapsed LCE was finally obtained as white disc floating in pure methanol. Subsequently, the network was dried at 40°C for two days and then at room temperature under vacuum for one day. The nematic network poly[6-(4′-cyanophenyl-4″-phenoxy) hexyl acrylate-co-1,6-hexanediol diacrylate] will be abbreviated as LCE-6OCB.

3.4 Thermal Analysis

Calorimetric measurements were carried out on a Mettler DSC 30 equipped with a liquid nitrogen system allowing cooling experiments. The DSC cell was purged with 50 ml/min of nitrogen. Data analysis was carried out on the second heating ramp using a ramp of 5°C/min for both polymer networks and solvents.

3.5 Polarized Optical Microscopy

The thermo-microscopy studies were performed on a Leitz polarized optical microscope (POM), equipped with a Linkam heating/cooling stage THMS 600 together with a temperature-controlling unit TMS 92. For the swelling measurements, thin sheets of dry polymer networks (thickness of approximately 50 μm) were sliced with a scalpel, cut into approximately 500 × 500 μm squares and placed in a THMS-Q quartz cell (Linkam Instruments), which allowed the thermo-microscopic observation of liquid samples without being sandwiched between two glass plates. The THMS-Q cell was filled with LMWLC and placed in the heating stage under a nitrogen atmosphere. Ratios of the gel dimensions (swollen/dry states) allow the precise determination of the swelling degree of the gel over a wide temperature range. The temperature was increased in a stepwise manner until the swollen polymer samples reached thermodynamic equilibrium at each given temperature.

3.6 Swelling Study

Sub-millimeter-sized samples with nearly rectangular shapes were prepared from the crosslinked poly (ABu/HDDA) and poly (LCE-6OCB/HDDA) networks. These samples were immersed in the LC solvents at room temperature for two days to enable the thermodynamic equilibrium state to be reached. Characterization was performed by observations via POM over a wide temperature range. Micrographs were taken at 5°C intervals until the swollen polymer samples reached thermodynamic equilibrium at each given temperature. Smaller temperature intervals were chosen in the vicinity of the nematic-isotropic phase transition temperatures of LC and nematic polymer. Six different ratios of length (l_1, l_2), width (w_1,w_2) and diagonals (d_1,d_2) (swollen to dry states) were collected as a function of temperature. Then, λ was defined as the average of these six ratios. The value λ is in fact the cubic root of the swelling ratio Q:

$$\lambda = Q^{1/3} = \frac{1}{6}\left(\frac{\lambda_{l_{1,0}}}{\lambda_{l_1}} + \frac{\lambda_{l_{2,0}}}{\lambda_{l_2}} + \frac{\lambda_{w_{1,0}}}{\lambda_{w_1}} + \frac{\lambda_{w_{2,0}}}{\lambda_{w_2}} + \frac{\lambda_{d_{1,0}}}{\lambda_{d_1}} + \frac{\lambda_{d_{2,0}}}{\lambda_{d_2}}\right) \tag{10}$$

For each polymer/5CB system, several samples were systematically measured and the shown values represent the average of results obtained from several samples prepared and analyzed under the same conditions.

4. Results and Discussion

Figure 1 shows thermograms from DSC measurements of polybutylacrylate (PABu)- and LCE-6OCB-polymer networks, crosslinked with 5wt% of HDDA. The LCE show two specific transition temperatures, a glass transition temperature (T_g) and a nematic-isotropic transition temperature (T_{NI}), whereas the PABu network exhibits only a glass transition temperature around −40°C.

In order to evaluate the influence of the nature of the polymer networks on the phase diagrams, the swelling properties of these networks were examined in a nematic solvent over a wide temperature range. The swelling behavior of these systems was followed by POM which allowed observing that the networks always swell homogeneously in all directions even in the liquid crystalline state. Figure 2 shows two representative swelling curves of the isotropic PABu and the mesogenic LCE-6OCB-networks, respectively.

In the first case, it is interesting to note that below the T_{NI} of 5CB, practically no swelling of the network occurred, but when the temperature increases gradually approaching T_{NI}, the swelling rate increases slowly. The swelling curve of the LCE-6OCB in the nematic solvent 5CB is quite different from the former one since it presents two distinct transition temperatures, the first one results from the LC solvent (dotted points), and the second one from the LC gel (dash-dotted points). For temperatures below T_{NI} of the LC solvent, the two components of the mixture (gel and solvent) are in the nematic state. In this temperature range, the swelling rate of the gel remains nearly constant. When approaching T_{NI} of 5CB

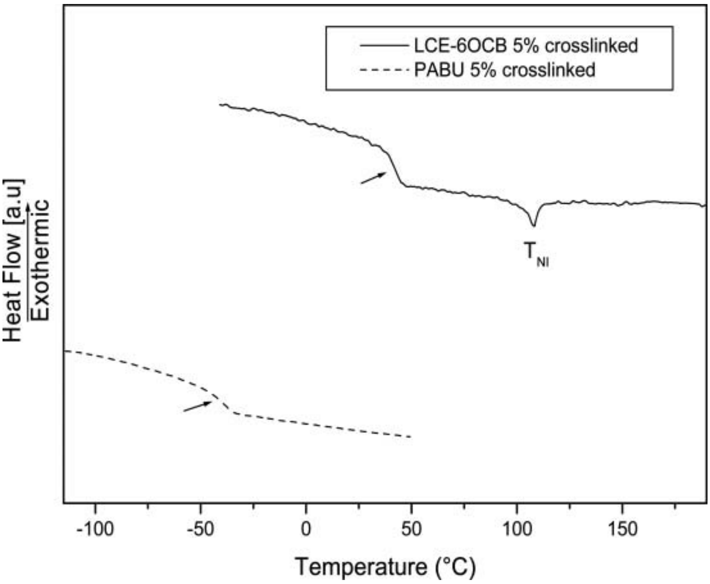

Figure 1. Thermograms from DSC measurements of PABu and LCE-6OCB polymer networks, crosslinked with 5wt% HDDA. The arrows indicate the glass transition temperatures (T_g), whereas the endothermic peaks correspond to the nematic-isotropic transition temperatures (T_{NI}).

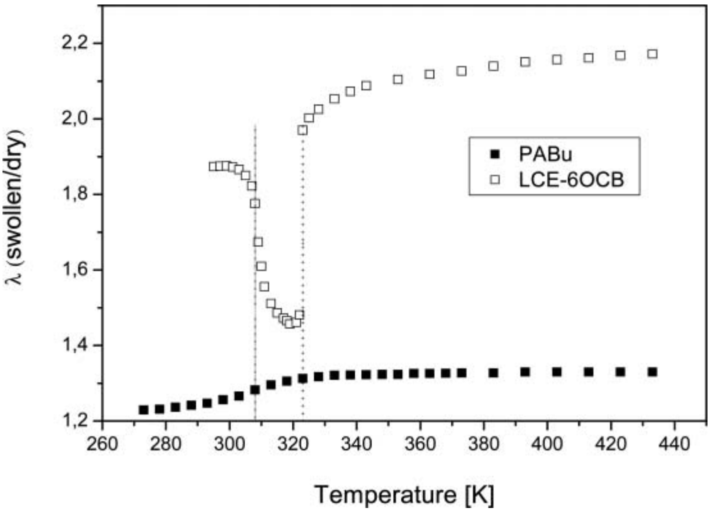

Figure 2. Evolution of the swelling rate of LCE-6OCB (empty points) and PABu (solid points) in the nematic solvent 5CB, according to the temperature. The dotted points correspond to the nematic-isotropic transition temperature of 5CB and the dash-dotted points stand for the nematic-isotropic transition temperature of the gel.

(35.3°C) by heating, the swelling rate starts to decrease. In the temperature range between the T_{NI} of solvent and gel, the excess of solvent has become isotropic while the gel is still nematic. The corresponding curve in Fig. 2 reaches a minimum for $T = 47.5°\text{C}$. Further increase of the temperature tends to depress the strength of anisotropic interactions inside the gel phase and results in shrinkage of the gel. The transition from the nematic gel state to the isotropic state ($T = 47.5°\text{C}$) results on a macroscopic scale by a large volume transition over a narrow temperature range, of about 0.5°C. This phase transition is quite specific to the molecular interactions governing these liquid crystalline interactions. From a practical point of view the coupling between the clusters of the LC network and those of the LC solvent represents a new molecular force in the field of smart materials.

The corresponding phase diagrams of PABu/5CB and LCE-6OCB/5CB systems are presented in Fig. 3. The symbols are experimental POM data and the LC volume fraction φ_{LC} was calculated from

$$\varphi_{LC} = 1 - (1/\lambda^3) \tag{11}$$

The phase diagram on the left hand side of Fig. 3 shows three distinct domains; isotropic, isotropic + isotropic and nematic + isotropic. On the right hand side of the same figure, the phase diagram of LCE-6OCB/5CB exhibits five domains, in relationship with two distinct temperatures 35°C and 50°C, corresponding respectively to the T_{NI} of 5CB and of the gel. The phase diagram shows in this case two monophasic and three biphasic domains.

Figure 4 displays micrographs obtained by POM observations showing the influence of swelling in the case of the isotropic network (Figs 4a–c) and the LCE-6OCB network (Figs 4d–f).

Figure 4a shows the sample immersed in 5CB at room temperature, under parallel polarizers. When the temperature reaches 27°C, the nematic character of 5CB appears (Fig. 4b); and further increase of temperature leads to the isotropic phase of the LC

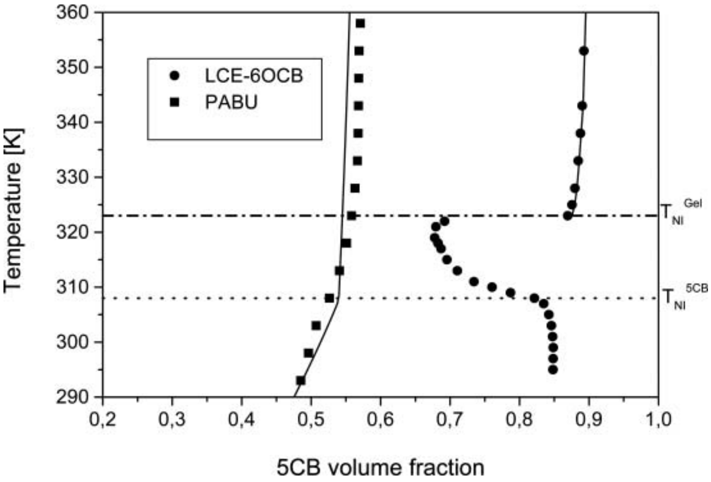

Figure 3. Phase diagrams of PABu/5CB and LCE-6OCB/5CB systems, obtained by POM. The solid lines represent the result of theoretical calculations of the isotropic binodals of the phase diagrams, using the parameters gathered in Table 1.

(Fig. 4c). Figure 4d presents the nematic network swollen in 5CB at 28°C. When the temperature increases exceeding T_{NI} of the nematic solvent, the nematic gel is surrounded by the isotropic solvent (Fig. 4e). A further increase of temperature leads to the isotropic phase of both gel and 5CB (Fig. 4f).

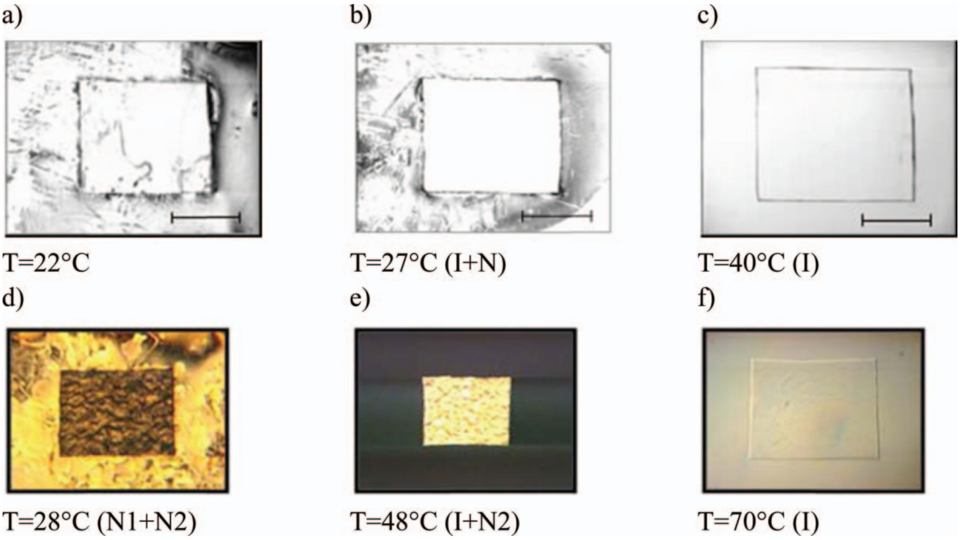

Figure 4. Optical micrographs showing the phase transitions of the isotropic network PABu and the nematic network LCE-6OCB swollen in 5CB. a) Isotropic PABu network at room temperature; b) Isotropic PABu network swollen in nematic solvent at 27°C; c) Isotropic PABu network swollen in isotropic 5CB at 40°C; d) Nematic LCE-6OCB network swollen in nematic 5CB at 28°C, e) Nematic LCE-6OCB gel surrounded by isotropic 5CB at 48°C; f) Isotropic state of LCE-6OCB and 5CB at 70°C. The scale bar corresponds to 500 μm.

The solid lines in Fig. 3 represent the results of theoretical calculations obtained starting from the combination of the theories of Flory-Rehner and Maier-Saupe. Indeed, thermodynamical equilibrium between two coexisting phases is determined by the equality of chemical potentials of each component in the two phases. For the nematic LC/crosslinked polymer system, a phase of swollen network or isotropic gel (α phase) is in equilibrium with a pure solvent phase (β phase). Thus the equilibrium is reached by equating the chemical potentials in the two phases (i.e. $\varphi_2^{(\beta)} = 0$ and $\mu_1^{(\alpha)} = \mu_1^{(\beta)} = 0$). Swelling of the network by the LC can occur either in the nematic phase ($T < T_{NI,}$ and $\varphi_1 < \varphi_{NI}$) or in the isotropic phase ($T > T_{NI,}$ and $\varphi_1 > \varphi_{NI}$). The quantity $\varphi_{NI} = T/T_{NI}$ represents the critical LC volume fraction below which nematic ordering does not exist.

The calculation of the binodal in the isotropic phase was obtained by differentiating the free energy with respect to the number of molecules which can be written in terms of f and its derivative with respect to φ_2:

$$\mu_1^{(i)} = f^{(i)} - \varphi_2 \frac{df^{(i)}}{d\varphi_2} \tag{12}$$

$$\mu_2^{(i)} = f^{(i)} - \varphi_1 \frac{df^{(i)}}{d\varphi_1} \tag{13}$$

The chemical potentials of the constituents should be balanced in equilibrium according to the equation:

$$\begin{cases} \mu_1^{(\alpha)} = \mu_1^{(\beta)} \\ \mu_2^{(\alpha)} = \mu_2^{(\beta)} \end{cases} \tag{14}$$

In the α phase, the condition $\varphi_1^{(\alpha)} = \varphi_1^{(\beta)}$is imposed. Similarly, in the β phase the condition is $\varphi_1^{(\beta)} = 1$; $\varphi_2^{(\beta)} = 0$. $\varphi_2^{(\beta)} = 0$ implies that the network cannot be dissolved by the LC solvent. For the LCE-6OCB/5CB system, only the isotropic part was considered since the model calculation of the phase diagram needs to take into account the effect of nematic coupling on the miscibility of polymer and solvent, which needs some more investigation. The results of the calculation procedures are given in Table 1.

Table 1. Results from theoretical calculations using Flory-Rehner and Maier Saupe theories, for PABu/5CB and LCE-6OCB/5CB systems. N_C represents the number of monomer units between two consecutive cross-links. The parameter χ will be assumed to be function of the temperature only $\chi = A + B/T$

Polymer network	PABu	LCE-6OCB
N_c	3	62
A	−0.07	−0.30
B	124	217

Conclusions

The preparation of samples of isotropic and LC polymer networks, swollen in a nematic LC (5CB), were considered in this work. Thin polymer films were immersed in an excess of 5CB, forming polymer gels. An extended study by POM allowed determining the swelling degree and the corresponding phase diagrams could be deduced for the polymer/LC systems. The phase behavior of LCE-6OCB swollen by 5CB exhibits an extended miscibility gap due to the anisotropic coupling between LC solvent molecules and LC side chains of the network. The influence of the nematic polymer backbone is considerable if it is compared to the isotropic polymer network. The theoretical analysis gives a good agreement for the isotropic part of the binodals of the phase diagrams. More investigations will be carried out to analyze theoretically the remaining domains of the phase diagram of the LCE-6OCB/5CB system.

References

[1] Rodriguez-Parada, J. M., & Percec, V. (1987). *J. Polym. Sci. Part A: Polym. Chem.*, *25*, 2269.
[2] Finkelmann, H., Ringsdorf, H., & Wendorff, J. H. (1978). *Makromol. Chem.*, *179*, 273.
[3] Ciferri, A., Krikbaum, W. R., & Meyer, R. B. (1982). *Polymer Liquid Crystals*, New York: Academic Press.
[4] Warner, M., & Terentjev, E. M. (2003). *Liquid Crystal Elastomers*, Oxford University Press: Oxford, UK.
[5] Sanchez-Ferrer, A., & Finkelmann, H. (2010). *Solid State Sciences*, *12*, 1849–1852.
[6] Giamberini, M., Ambrogi, V., Cerruti, P., & Carfagna, C. (2006). *Polymer*, *47*, 4490–4496.
[7] Misra, G., & Srivastava, A.K. (2008). *Colloid Polym. Sci.*, *286*, 445–451.
[8] Zhang, B., Hu, J., Wang, B., Yao, D., & Li, H. (2007). *Colloid Polym. Sci.*, *285*, 1683–1690.
[9] Hu, J., Zhang, B., Zhou, A., Yang, L., & Wang, B. (2006). *Eur. Polym. J.*, *42*, 2849–2858.
[10] Finkelmann, H., Kock, H. J., & Rehage, G. (1981). *Makromol. Chem., Rapid Commun.*, *2*, 317.
[11] Zentel, R., & Reckert, G. (1986). *Macromol. Chem.*, *87*, 1915.
[12] Shivakumar, E., Das, C. K., Segal, E., & Narkis. M. (2005). *Polymer*, *46*, 3363.
[13] Saikrasun, S., Bualek-Limcharoen, S., Kohjiya, S., & Urayama, K. (2005). *J. Polym. Sci., Part B: Polym. Phys.*, *43*, 135.
[14] Halperin, A., & Williams, D. R. M. (1994). *J. Phys. Condens. Matter*, *6*, 297.
[15] Lange, H., & Schmid, E. (2002). *Eur. Phys. J.*, *E7*, 175.
[16] Lange, H., & Schmid, E. (2002). *J. Chem. Phys.*, *117*, 362.
[17] Brochard-Wyart, F., Ramdane, Ou. O., Tran, Y., & Auroy, P. (2003). *Macromol. Symp.*, *191*, 59.
[18] Dowtown, M. T., & Allen, M. P. (2004). *Europhys. Lett.*, *65*, 48.
[19] Peng, B., Rüke, J., & Johannsmann, D. (2000). *Adv. Mater.*, *12*, 821.
[20] Benmouna, F., Peng, B., Gapinski, J., Patkowski, A., Rühe, J., & Johannsmann, D. (2001). *Liq. Cryst.*, *28*, 1353.
[21] Spillmann, C. M., Naciri, J., Martin, B. D., Farahat, W., Herr, H., & Ratna, B. R. (2007). *Sensors and Actuators A*, *133*, 500.
[22] Binet, C., Bourrier, D., Dilhan, M., Estève, D., Ferrère, S., Garrigue, J. C., Granier, H., Lattes, A., Gué, A. M., Mauzac, M., & Mingotaud, A. F. (2006). *Talanta*, *69*, 757.
[23] Dusek, K. (1993). Advances In Polymer Science, *Responsive gels: volume transitions I*, 109.
[24] Amoskov, V. M., & Birshtein, T. M. (2010). *Polym. Sci. Ser. C.*, *52*, 44.
[25] Lacoste, D., Lau, A. W. C., & Lubensky, T. C. (2002). *Eur. Phys. J.*, *8*, 403.
[26] Flory, P. J., & Rehner, R. (1993). *J. Chem. Phys.*, *11*, 521.
[27] Maier, W., & Saupe, A. (1960). *Z. Naturforschung.*, *15a*, 287.
[28] De Gennes, P. G., & Prost, J. (1994). *The Physics of Liquid Crystals*, Oxford Science Publications: Oxford, U.K.
[29] Kyu, T., & Chiu, H. W. (1996). *Phys. Rev. E.*, *53*, 3618.

[30] Chiu, H. W., & Kyu, T. (1997). *J. Chem. Phys.*, *107*, 6859.

[31] Chiu, H. W., & Kyu, T. (1998). *J. Chem. Phys.*, *108*, 3249.

[32] Benmouna, F., Coqueret, X., Maschke, U., & Benmouna, M. (1998). *Macromolecules*, *31*, 4879.

[33] Briber, R. M., & Bauer, B. J. (1991). *Macromolecules*, *24*, 1899.

[34] Kumar, S. (1995). *Liquid Crystals in The Nineties and Beyond*, Word Scientific, Singapore.

[35] James, H., & Guth, E. J. (1947). *J. Chem. Phys.*, *15*, 669.

[36] Flory, P. J. (1950). *J. Chem. Phys.*, *18*, 108.

[37] Petrovic, Z. S., MacKnight, W. J., Koningsveld, R., & Dusek, K. (1987). *Macromolecules*, *20*, 1088.

[38] Shibaev, V. P., Kostromin, S. G., & Plate, N. A. (1982). *Eur. Polym. J.*, *18*, 651.

[39] Kishi, R., Kitano, T., & Ichijo, H. (1996). *Mol. Cryst. Liq. Cryst.*, *280*, 109.